Article

Research on Hard, Transparent and Hydrophobic Coating on PMMA Sheet

Guoqing Wu [1,2,*], Xiaoping Chen [1,2], Xuanyu Xie [3], Pu Zhang [1,2], Shenyu Ge [1], Wei Chen [1], Xian Zeng [3,*] and Ruoye Wang [1]

1   China Ship Scientific Research Center, Wuxi 214000, China
2   Taihu Laboratory of Deepsea Technological Science, Wuxi 214082, China
3   School of Materials Science and Engineering, Wuhan University of Technology, Wuhan 430070, China
*   Correspondence: 15852797071@139.com (G.W.); zengxian9925@163.com (X.Z.)

Featured Application: This technology can realize self-cleaning of deep-sea optical windows, reducing the cost of equipment maintenance and cleaning.

Abstract: In this paper, nano SiO_2 particles modified organic silane coatings were successfully prepared to aim at the application of the self-cleaning coating on PMMA substrate for deep-sea optical windows. The chemicals, surface microstructure, wettability, hardness, adhesion, transparency, water scouring resistance as well as microorganism attachment rate of the coatings were investigated. The results showed that adding SiO_2 nanoparticles into the organic silicon coating can effectively improve the hydrophobicity due to generating a micro-nano structure surface. However, excessive addition would result in a decrease in hydrophobicity, adhesion, as well as transparency, due to the inorganic SiO_2 particle destroying the integrity of the organic coating. The optimal coating was obtained by adding 0.5 wt% nano SiO_2 particles, which possessed a water contact angle of 114.2°, hardness of 4H, adhesion level of 0, and visible light transmittance of 0.886. After 40-h water scouring, the water contact angle decreased to 108.3° and the visible light transmittance decreased to 0.839, suggesting good water scouring resistance. The microorganism attachment rate of the S05 coating was 0.17% after a 6 h immersion test, which was about half that of the PMMA substrate.

Keywords: self-cleaning coating; wettability; hardness; adhesion; transparency; water scouring

1. Introduction

Polymethyl methacrylate (PMMA), generally known as plexiglass, is wildly used for optical windows material due to its good light transmission performance, high mechanical strength, good corrosion resistance and easy molding [1]. However, the surface of light-transmitting materials of underwater optical windows will be affected by various factors such as seawater erosion, corrosion and marine biological fouling, which seriously interferes with the performance and stability of underwater optical equipment. By coating self-cleaning coating on the surface of window materials, the cost of equipment maintenance and cleaning can be effectively reduced.

Common self-cleaning coatings are mainly divided into two categories. One is hydrophobic coating with low surface energy, which is mainly composed of organic silane coating [2–4] and organic fluorine coating [5–7], and the other is photocatalytic coating containing TiO_2 [8–10]. It is worth mentioning that the self-cleaning coating applied to the PMMA surface in the above environment needs to meet several characteristics. In addition to good self-cleaning effects, the light transmission, adhesion strength and wear resistance of the coating must also be considered. More importantly, the heat resistance of polymethylmethacrylate is not high. Although its glass transition temperature reaches 104 °C, the maximum continuous use temperature varies from 65 to 95 °C depending on the working conditions, and the thermal deformation temperature is about 96 °C. Therefore,

the forming temperature of self-cleaning coating shall not exceed 60 °C, and it is better to have the ability of cure at room temperature.

Contributed to good adhesion, hydrophobicity and corrosion resistance, organic silane coating is an ideal material for preparing self-cleaning coating. Moreover, it also can be formed at room temperature by adjusting the composition of the siloxane monomer [11]. Among the commonly used alkoxysilane monomers, methyltrialkoxysilane and orthosilicate are beneficial to hardness due to high crosslinking, and dimethyldialoxysilane is beneficial to hydrophobicity. In addition, inspired by the lotus leaves, a superhydrophobic surface can be achieved by a combination of low surface energy materials and micro-nanostructures [12–15]. Thus, in this paper, targeting the self-cleaning coating of PMMA optical window, we prepared a hard, transparent and hydrophobic coating by using methyltrialkoxysilane, orthosilicate and dimethyldialoxysilane as the raw material for organic silane coating and nano-silica as a modifier. The chemicals, surface microstructure, wettability, hardness, adhesion, transparency, water scouring resistance as well as microorganism attachment rate of the coatings were systematically investigated in this study, which might provide a new way to solve the problem of deep-see contamination of optical windows.

2. Materials and Methods

2.1. Coatings Preparation

PMMA sheet with a size of 30 mm × 40 mm × 3 mm was used as substrate. Tetraethoxysliane (TEOS), methyltriethoxysilane (MTES), Dimethoxydimethylsilane (DMDS) were used as the precursor of silicon source. Absolute ethanol was used as a solvent. 3–(isobutenyloxy) propyltrimethoxysilane (KH570) was used as a coupling agent. Hydrophobic nano SiO_2 particles (size ranging 7–40 nm) were used as a surface modifier, and the added amounts were 0 (S0), 0.5 wt% (S05), 1 wt% (S1), 2 wt% (S2) correspondingly. Hydrochloric acid (HCl, 37 wt%) was used as a catalyst. The absolute ethanol and hydrochloric acid were purchased from China National Pharmaceutical Group Co., Ltd. (Beijing, China). The rest chemicals were purchased from Shanghai Macklin Biochemical Technology Co., Ltd. (Shanghai, China).

Firstly, the nano SiO_2 particles were ultrasonically dispersed with absolute ethanol for 30 min. Then TEOS, MTES and DMDS with a mole ratio of 3:5:2 were added into the dispersion and mixed for 1 h. After that, a proper amount of deionized water and hydrochloric acid were added to the solution and fully mixed for 1 h at 70 °C, and then cooled to room temperature. Finally, the self-cleaning paint was obtained by adding the coupling agent KH570 and mixing it for 6 h at room temperature. A top pot spray gun was employed to deposit the coating on the PMMA substrate with an air pressure of 28 kPa. The sprayed sample was cured at room temperature for 24 h, pending testing.
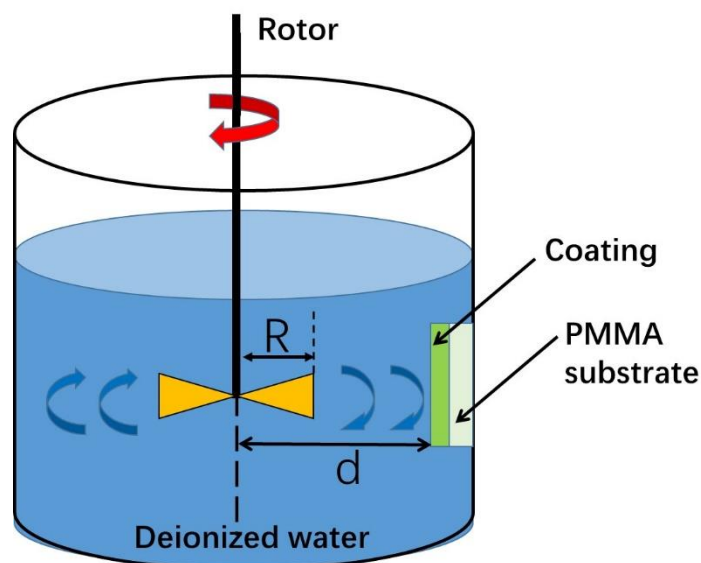
2.2. Characterizations

Use a standard contact angle tester (SL-200A, Kono, USA) to measure the wetting angle of the self-cleaning coating, use a UV-VIS-NIR spectrometer (UV3600, Tsushima, Japan) to measure the visible light transmittance of the coating, and use a Fourier transform infrared spectrometer (FTIR, Nicolet6700, Thermophile, USA) to measure the infrared spectrum of the coating. Use a cold field emission scanning electron microscope (SEM, JSM-7500F, Japan Electronics Co., Ltd.) to observe the microstructure of the coating surface, use a hand-pushed pencil hardness tester (QHQ-A, Zhejiang Aipu) to measure the hardness of the coating according to ISO 15184:2020 Paints and Varnishes-Determination of Film Hardness by pencil test, and use a Baige knife (QFH-A, Zhejiang Airuipu) to measure the adhesion of the coating according to ISO 2409:2020 Paints and Varnishes-Cross-Cut Test. The judgment standards of coating adhesion are shown in Table 1.

Table 1. Classification of test results for coating adhesion.

Classification	Description
0	The edges of the cuts are completely smooth; none of the squares of the lattice is detached.
1	Detachment of small flakes of the coating at the intersections of the cuts. A cross-cut area not greater than 5% is affected.
2	The coating has flaked along the edges and/or at the intersections of the cuts. A cross-cut area greater than 5%, but no greater than 15%, is affected.
3	The coating has flaked along the edges of the cuts partly or wholly in large ribbons, and/or it has flaked partly and wholly on different parts of the squares. A cross-cut area greater than 15%, but not greater than 35%, is affected.
4	The coating has flaked along the edges of the cuts in large ribbons and/or some squares have detached partly or wholly. A cross-cut area greater than 35%, but not greater than 65%, is affected.
5	Any degree of flaking that cannot even be classified by classification 4.

The water-flow scouring resistance of the prepared coating was evaluated through a laboratory self-made test device as shown in Figure 1, where the rotor stirred the deionized water to form an annular flow. The coating sample was fixed at the same height level as the rotor blades, and the coating surface was perpendicular to the radial direction. The rotor radius R was 40 mm, and the distance d from the coating surface to the axis was 50 mm. The rotor speed was 2000 rad/min. The wettability and transparency after 20 h and 40 h scouring were detected.
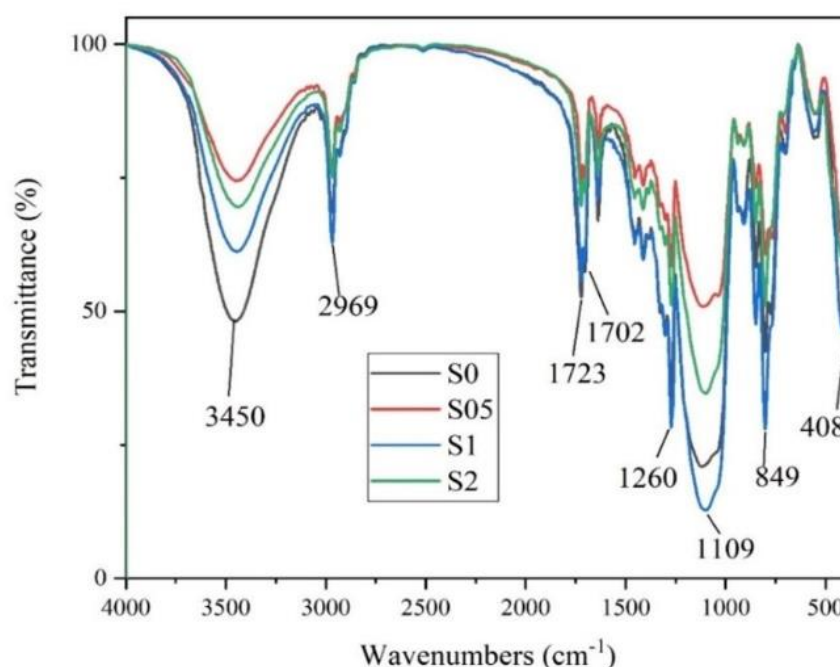

Figure 1. Schematic diagram of water-flow scouring test.

The microorganism attachment behavior of the prepared coating was evaluated by a microbial immersion test. Specifically, immerse the sample in sterilized seawater for 12 h, and then take it out and immerse it in the phaeodactylum tricornutum solution with a concentration of 2×10^6 for 6 h. After the immersion test, the sample surface is washed with ultrapure water for 30 s. The microorganism attachment rate is calculated by counting the adhesion area rate with a fluorescence microscope (FM, ZEISS, Germany). A total of 20 random fields magnified by 40 times were taken by the fluorescence microscope for each sample. The adhesion area was evaluated via an Image processing software (Image pro-plus).
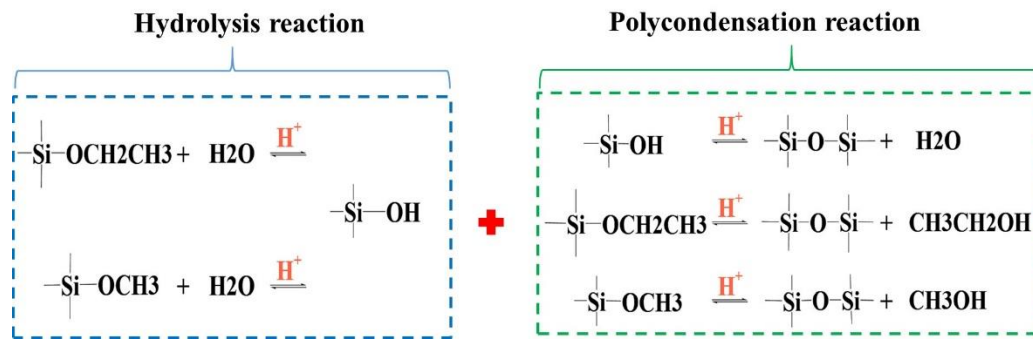
3. Results and Discussions

3.1. Chemicals of Coatings

In order to identify the chemicals of prepared coatings, infrared spectral analysis was performed and the results are shown in Figure 2. It was seen that all the coatings exhibited similar infrared spectrums. The main absorption peaks located at $3450 \ cm^{-1}$ and $1109 \ cm^{-1}$ belonged to the vibrations of Si-OH and Si-O-Si correspondingly, indicating most siloxanes had been hydrolyzed and polycondensation. The peak at $2969 \ cm^{-1}$, $1260 \ cm^{-1}$ and $849 \ cm^{-1}$ belonged to the stretching vibrations of Si-O-C_2H_5 [16], suggesting insufficient hydrolysis of siloxane monomer. Specifically, the peak at $2969 \ cm^{-1}$ was related to the C-H stretching vibration of residual CH_3 from non-hydrolyzed Si-O-C_2H_5 groups, and the small peaks near and below $2969 \ cm^{-1}$ were assigned to asymmetric and symmetric C-H vibrations of CH_2. Moreover, the peaks between $1500–1260 \ cm^{-1}$ were assigned to various C-H vibrations, and around $849 \ cm^{-1}$ with a band of $900–750 \ cm^{-1}$ were assigned to CH_2 [17] Due to the addition of KH570, the vibration absorption peaks of olefin stretching ($1702 \ cm^{-1}$) and C=O ester contraction ($1723 \ cm^{-1}$) were also observed [18]. The peaks located in $400–500 \ cm^{-1}$ belonged to the absorption peaks of Si-O-Si [19].

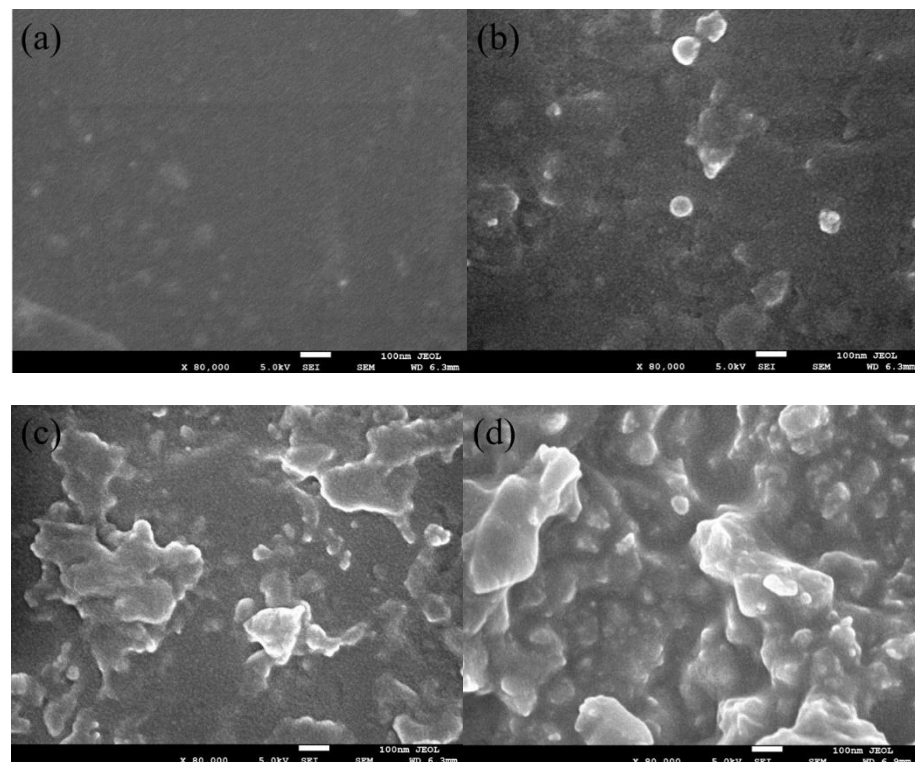**Figure 2.** Infrared spectra of nano SiO_2 particles modified coatings with different weight ratio.

In an acid environment, the alkoxysilane monomers would undergo hydrolysis and condensation reactions according to Figure 3. Organic groups (methyl, phenyl, etc.) directly linked to silicon atoms do not participate in the hydrolysis and condensation reactions, while the main one involved in the reaction process is oxyethyl and oxymethyl. When using acid as a catalyst, H^+ attacks -OCH_2CH_3 and/or -OCH_3 groups and results in the protonation and the shift of extranuclear electron cloud to it, weakening the Si-O bond until it breaks and forms Si-OH. So far, one-step hydrolysis has been completed. After hydrolysis, the generated Si-OH will further participate in the condensation reaction with Si-OH, Si-OCH_2CH_3 and Si-OCH_3 under the catalyst action of acid, forming a three-dimensional network structure of Si-O-Si, water and alcohol substance. It is worth noting that although a single monomer is hydrolyzed first and then condensed, hydrolysis and condensation occur simultaneously in the whole system, so incomplete hydrolysis may occur.

Hydrolysis reaction

Polycondensation reaction

Figure 3. Schematic diagram of hydrolysis and condensation reactions of alkoxysilane monomers.

3.2. Surface Morphology of Coatings

The surface morphology of prepared coatings is shown in Figure 4. It was found that the surface of organic silicon coating without nano SiO_2 particles was relatively smooth and homogeneous. However, the surface of coatings after modification became rougher and rougher as increasing the amount of nano SiO_2 particles. The micro-bulge structure was formed by introducing nanoparticles, which increased the surface roughness apparently. Furthermore, no cracks or pores were observed on the surface, indicating good compatibility between nanopowders and base materials. However, the agglomeration of nano SiO_2 particles occurred properly, owing to the insufficient dispersion of SiO_2, where the sizes of those micro-bulge structures were much larger than that of a single nanoparticle.
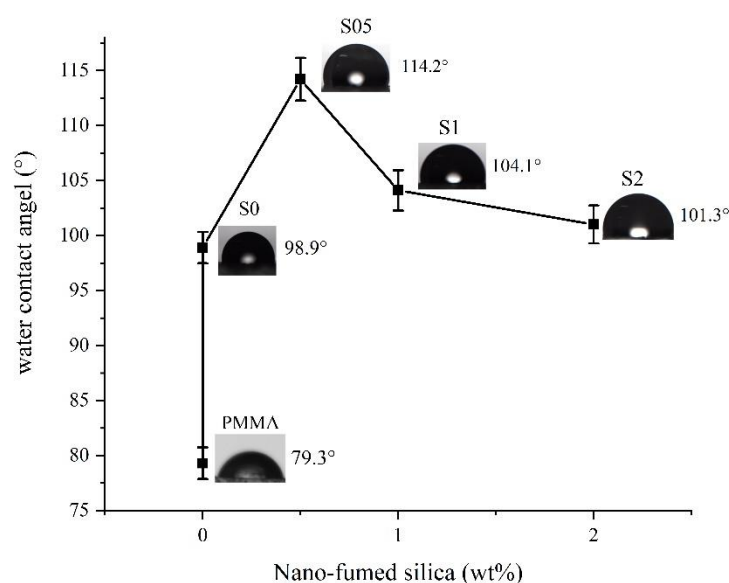

Figure 4. Surface morphology of nano SiO_2 particles modified coatings with different weight ratio (**a**) 0, (**b**) 0.5 wt%, (**c**) 1 wt%, and (**d**) 2 wt%.

3.3. Wettability of Coatings

The wettability of the coating was evaluated by testing the average water contact angle of five samples. The wettability of coatings against nano SiO_2 content is shown in Figure 5. According to it, the average water contact angle of bare PMMA substrate was 79.3°, while after coating, the surface water contact angle was improved above 100°

showing hydrophobic properties. The greatest average water contact angle was 114.2° when the coating was modified with 0.5 wt% nano SiO_2 particles. However, the water contact angle decreased when the amount of SiO_2 continued to increase. It is generally accepted that surface micro-nano structure improves the hydrophobicity, which works similarly to lotus leaves. On the one hand, this contributed to the low surface energy of silicone coating and the micro-nano structure induced by nano SiO_2 particles, the surface water contact angle of PMMA increased after coating and showed hydrophobic properties, which can reduce the adhesion of marine microorganisms or make the pollutants easy to clean by seawater. On the other hand, due to the physical absorption of water on the SiO_2 particle surface [20], the water contact angle would decrease when massive nano SiO_2 particles were added.

Figure 5. Water contact angles of samples with different nano SiO_2 particles.

3.4. Hardness and Adhesion of Coatings

The hardness of PMMA substrate and coatings was tested according to ISO 15184:2020 Paints and Varnishes-Determination of film hardness by pencil test. The pencil is tilted at 45° to the coating by the hand-pushed pencil hardness tester, and the load applied on the coating surface by the tip of the pencil is 750 g. The cross-cut method was used to detect the adhesion of coatings according to the ISO 2409:2020 Paints and Varnishes-Cross-Cut test. During the test, six parallel cuts are introduced in the coating by the multi-blade cutting tool, and then another six cuts are introduced perpendicular to the first cuts. The spacing of cuts was set as 1 mm. before qualifying the adhesion levels, the loose particles of coatings were removed by brushing and using pressure-sensitive adhesive tape. The detected results of coating hardness and adhesion are listed in Table 2.

Table 2. Hardness and adhesion levels of PMMA and coatings.

Samples	Hardness	Adhesion *Levels*
PMMA	*B*	-
S0	*4H*	0
S05	*4H*	0
S1	*4H*	0
S2	*4H*	1

As shown, the hardness of the coating was higher than the that of PMMA substrate, suggesting better wear resistance of the coating samples. In addition, the added amounts of nano SiO_2 particles were too low to have effects on the coating hardness, which showed
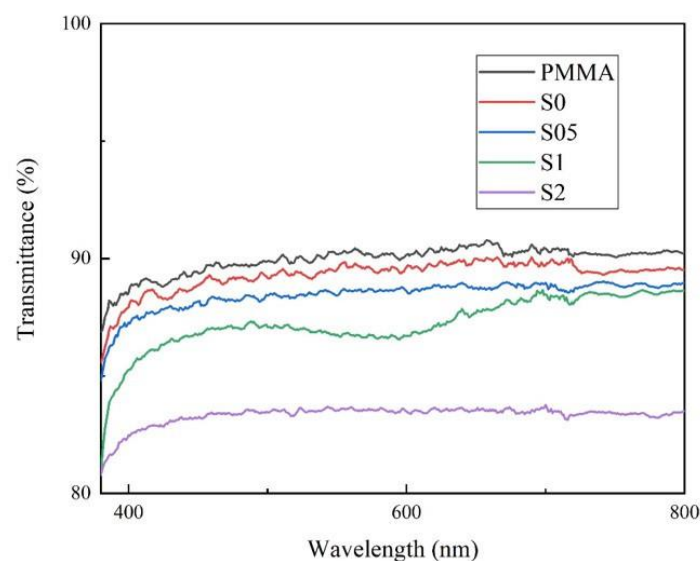
the same hardness of 4H. However, the adhesion of the S2 coating was worse than the other coatings, showing an adhesion level of 1. The continuity and integrity of the organic coating would be destroyed by adding inorganic SiO_2 particles, generating more interfaces, which might develop into crack sources, thus reducing the adhesion of the coating.

3.5. Transparency of Coatings

The spectrum transmittance of PMMA and coatings modified with different nano SiO_2 particle weight ratios in the wavelengths of 380 nm–800 nm was detected and shown in Figure 6. It was found that the spectrum transmittance of the coatings was lower than the substrate in the whole band. In addition, the transmittance declined with the increasing weight ratio of SiO_2 due to the scattering of nanoparticles. The total transmittance of samples in 380 nm~800 nm was calculated according to the following equation based on JISR 3106-2019.

$$\tau_v = \frac{\sum_\lambda D\lambda \cdot V\lambda \cdot \tau(\lambda)}{\sum_\lambda D\lambda \cdot V\lambda}$$

where τ_v is visible light transmittance, $D\lambda$ is the relative spectral energy distribution of CIE daylight D_{65}, $V\lambda$ is CIE light adaptation relative luminous efficiency, $\tau(\lambda)$ is the spectrum transmittance. The calculated results are listed in Table 3. It was found that the lowest visible light transmittance 0.835 was obtained with the S2 coating, which was only decreased by 7.3% as compared to that of bare PMMA substrate, suggesting good transparency of the prepared coatings.

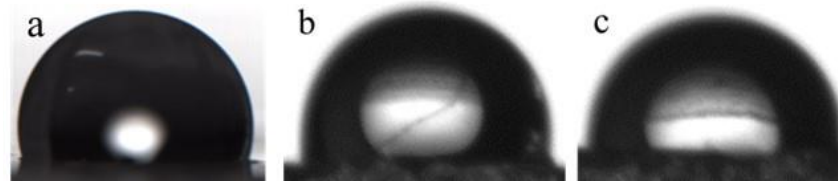**Figure 6.** Visible light transmission spectra of PMMA and nano SiO_2 particles modified coatings.

Table 3. Visible light transmittance of PMMA and coatings.

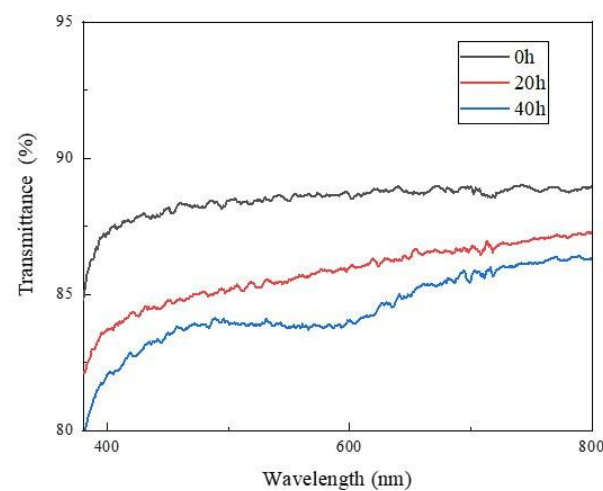| Samples	PMMA	S0	S05	S1	S2
τ_v (%)	90.1	89.5	88.6	86.9	83.5

3.6. Scouring Resistance of Coatings

Relating to the wettability, hardness, adhesive strength and transparency of the coatings comprehensively, the S05 coating was chosen as the optimal coating and underwent the water scouring test. As shown in Figure 7, the wettability of the coating slightly increased, where the water contact angles were 110.6° after 20 h and 108.3° after 40 h. The visible light transmission spectra of the S05 coating after the scouring test are shown in Figure 8, implying that the spectral transmittance was decreased in the whole observed wave band. The total visible light transmittance of the coating was 85.6% after 20 h and 83.9% after

40 h, correspondingly. The roughness of the coating surface increased with increasing the scouring time, which reduced the transparency of the coating. Meanwhile, the coating surface area increased, which promoted the wetting behavior between the water drop and the coating.
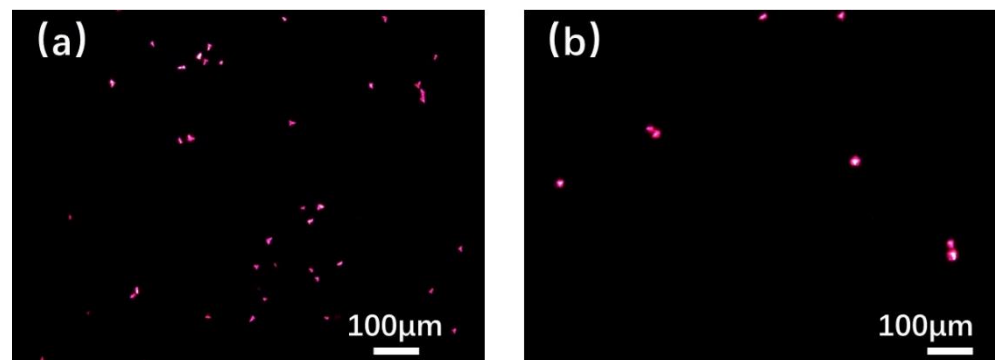

Figure 7. Water contact angles of S05 coatings with different scouring time (**a**) 0 h, (**b**) 20 h, and (**c**) 40 h.

Figure 8. Visible light transmission spectra of S05 coatings with different scouring time.

3.7. Microrganism Attachment Rate of Coatings

The microorganism attachment rates of the PMMA substrate and the S05 coating were measured by counting the mean attachment area ratio of 20 random fields magnified by 40 times. As shown in Figure 9, the attachment area (indexed by pink color) of phaeodactylum tricornutum on the PMMA substrate was apparently larger than that of the S05 coating. Attributed to a better hydrophobicity, the attachment of phaeodactylum tricornutum on the coating surface was weaker and easier to wash away by the water flow. The calculated microorganism attachment rate of the S05 coating was 0.17%, which was about half that of the PMMA substrate.

Figure 9. FM images of samples after microorganism immersion test for (**a**) PMMA sheet and (**b**) S05 coating.

4. Conclusions

In this paper, targeting the application of a self-cleaning coating on PMMA substrate for deep-sea optical windows, nano SiO_2 particles modified organic silane coatings were successfully prepared. The chemicals, surface microstructure, wettability, hardness, adhesion, transparency, water scouring resistance as well as microorganism attachment behavior of the coatings were investigated. The results showed that adding SiO_2 nanoparticles into the organic silicon coating can effectively improve the hydrophobicity due to generating a micro-nano structure surface. However, excessive addition would result in a decrease in hydrophobicity, adhesion as well as transparency, due to the inorganic SiO_2 particle destroying the integrity of the organic coating. The optimal coating was the S05 coating, which possessed a water contact angle of 114.2°, hardness of 4H, adhesion level of 0, and visible light transmittance of 0.886. After 40-h water scouring, both the water contact angle and the visible light transmittance were slightly decreased, which were 108.3° and 0.839 respectively, implying good water scouring resistance. Moreover, the microorganism attachment rate of the S05 coating was about half that of the PMMA substrate, suggesting good application prospects for deep-sea optical windows.

References

1. Xia, F.; Yang, L.; Dai, B.; Gao, G.; Yang, Z.; Cao, W.; Xu, L. Novel reparation method for polymethyl methacrylate optical windows of aircrafts damaged by service environment. *Sci. China Technol. Sci.* **2016**, *101*, 385–390. [CrossRef]
2. Matin, A.; Merah, N.; Ibrahim, A. Superhydrophobic and self-cleaning surfaces prepared from a commercial silane using a single-step drop-coating method. *Prog. Org. Coat.* **2016**, *99*, 322–329. [CrossRef]
3. Adark, D.; Bhattacharyya, R.; Saha, H.; Maiti, P.S. Sol–gel processed silica based highly transparent self-cleaning coatings for solar glass covers. *Mater. Today Proc.* **2020**, *33*, 2429–2433. [CrossRef]
4. Kumar, D.; Wu, X.; Fu, Q.; Weng, J.; Ho, C.; Kanhere, P.D.; Li, L.; Chen, Z. Development of durable self-cleaning coatings using organic-inorganic hybrid sol-gel method. *Appl. Surf. Sci.* **2015**, *344*, 205–212. [CrossRef]
5. Cui, Y.; Wei, B.; Wang, Y.; Guo, X.; Xiao, J.; Li, W.; Pang, A.; Bai, Y. Fabrication of UV/moisture dual curing coatings based on fluorinated polyoxetanes for anti-fouling applications. *Prog. Org. Coat.* **2022**, *163*, 106656. [CrossRef]
6. Yu, F.; Gao, J.; Liu, C.; Chen, Y.; Zhong, G.; Hodges, C.; Chen, M.; Zhang, H. Preparation and UV aging of nano-SiO2/fluorinated polyacrylate polyurethane hydrophobic composite coating. *Prog. Org. Coat.* **2020**, *141*, 10556. [CrossRef]
7. Kumar, D.; Li, L.; Chen, Z. Mechanically robust polyvinylidene fluoride (PVDF) based superhydrophobic coatings for self-cleaning applications. *Prog. Org. Coat.* **2016**, *101*, 385–390. [CrossRef]
8. Xu, F.; Wang, T.; Chen, H.; Bohling, J.; Maurice, A.M.; Wu, L.; Zhou, S. Preparation of photocatalytic TiO2-based self-cleaning coatings for painted surface without interlayer. *Prog. Org. Coat.* **2017**, *113*, 15–24. [CrossRef]
9. Chen, P.; Wei, B.; Zhu, X.; Gao, D.; Gao, Y.; Cheng, J.; Liu, Y. Fabrication and characterization of highly hydrophobic rutile TiO2-based coatings for self-cleaning. *Ceram. Int.* **2019**, *45*, 6111–6118. [CrossRef]
10. Zong, L.; Wu, Y.; Li, X.; Jiang, B. The preparation of superhydrophobic photocatalytic fluorosilicone/SiO2–TiO2 coating and its self-cleaning performance. *J. Coat. Technol. Res.* **2021**, *18*, 1245–1259. [CrossRef]
11. Zhan, Y.; Grottenmüller, R.; Li, W.; Javaid, F.; Riedel, R. Evaluation of mechanical properties and hydrophobicity of room-temperature, moisture-curable polysilazane coatings. *J. Appl. Polym. Sci.* **2021**, *138*, 50469. [CrossRef]
12. Jeevahan, J.; Chandrasekaran, M.; Britto Joseph, G.; Durairaj, R.B.; Mageshwaran, G. Superhydrophobic surfaces: A review on fundamentals, applications, and challenges. *J. Coat. Technol. Res.* **2018**, *15*, 231–250. [CrossRef]
13. Bhushan, B.; Multanen, V. Designing liquid repellent, icephobic and self-cleaning surfaces with high mechanical and chemical durability. *Philos. Trans. R. Soc. A Math. Phys. Eng. Sci.* **2019**, *377*, 20180270. [CrossRef] [PubMed]

14. Hooda, A.; Goyat, M.S.; Pandey, J.K.; Kumar, A.; Gupta, R. A review on fundamentals, constraints and fabrication techniques of superhydrophobic coatings. *Prog. Org. Coat.* **2020**, *142*, 105557. [CrossRef]

15. Farzaneh, M. Ice accretions on high-voltage conductors and insulators and related phenomena. *Philos. Trans. R. Soc. A Math. Phys. Eng. Sci.* **2000**, *358*, 2971–3005. [CrossRef]

16. Hu, C.; Xu, G.; Shen, X.; Shao, C.; Yan, X. The epoxy-siloxane/Al composite coatings with low infrared emissivity for high temperature applications. *Appl. Surf. Sci.* **2010**, *256*, 3459–3463. [CrossRef]

17. Öhman, M.; Persson, D. ATR-FTIR Kretschmann spectroscopy for interfacial studies of a hidden aluminum surface coated with a silane film and epoxy I. Characterization by IRRAS and ATR-FTIR. *Surf. Interface Anal.* **2012**, *44*, 133–143. [CrossRef]

18. Peng, C.; Wu, Z.; Li, J.; Wang, Z.; Wang, H.; Zhao, M. Synthesis, thermal and mechanical behavior of a silicon/phosphorus containing epoxy resin. *Appl. Polym.* **2015**, *132*, 1–10. [CrossRef]

19. Du, Y.; Wang, C.; Yang, L.; Zhu, S.; Wang, F. Enhanced oxidation and corrosion inhibition of 1Cr11Ni2W2MoV stainless steel by nano-modified silicone-based composite coatings at 600 °C. *Corros. Sci.* **2020**, *169*, 108599. [CrossRef]

20. Machia, M.; Norimoto, K.; Watanabe, T.; Hashimoto, K.; Fujishima, A. The effect of SiO_2 addition in super-hydrophilic property of TiO_2 photocatalyst. *J. Mater. Sci.* **1999**, *34*, 2569–2574. [CrossRef]